

SSC-126

**INFLUENCE OF HOT-ROLLING CONDITIONS ON  
BRITTLE FRACTURE IN STEEL PLATE**

by  
F. de Kazinczy  
and  
W. A. Backofen

SHIP STRUCTURE COMMITTEE

# SHIP STRUCTURE COMMITTEE

## MEMBER AGENCIES:

BUREAU OF SHIPS, DEPT. OF NAVY  
MILITARY SEA TRANSPORTATION SERVICE, DEPT. OF NAVY  
UNITED STATES COAST GUARD, TREASURY DEPT.  
MARITIME ADMINISTRATION, DEPT. OF COMMERCE  
AMERICAN BUREAU OF SHIPPING

## ADDRESS CORRESPONDENCE TO:

SECRETARY  
SHIP STRUCTURE COMMITTEE  
U. S. COAST GUARD HEADQUARTERS  
WASHINGTON 25, D. C.

November 10, 1960

Dear Sir:

Herewith is a copy of SSC-126 entitled Influence of Hot-Rolling Conditions on Brittle Fracture in Steel Plate by F. de Kazinczy and W. A. Backofen. This is the first progress report of a project sponsored by the Ship Structure Committee at the Massachusetts Institute of Technology to determine the relationship of mill-rolling practice to metallurgical structure and properties of ship plate.

The work has been conducted under the advisory guidance of the Committee on Ship Steel of the National Academy of Sciences-National Research Council.

This report is being distributed to individuals and groups associated with and interested in the work of the Ship Structure Committee. Please submit any comment that you may have to the Secretary, Ship Structure Committee.

Sincerely yours,



E. H. THIELE  
Rear Admiral, U. S. Coast Guard  
Chairman, Ship Structure Committee

Serial No. SSC-126

First Progress Report  
of  
Project SR-147

to the

SHIP STRUCTURE COMMITTEE

on

INFLUENCE OF HOT-ROLLING CONDITIONS ON  
BRITTLE FRACTURE IN STEEL PLATE

by

F. de Kazinczy

Oxelösunds Järnverksaktiebolag  
Oxelösund, Sweden

W. A. Backofen

Massachusetts Institute of Technology  
Cambridge, Massachusetts

under

Department of the Navy  
Bureau of Ships Contract NObs-72386  
BuShips Index No. NS-011-078

transmitted through

Committee on Ship Steel  
Division of Engineering and Industrial Research  
National Academy of Sciences-National Research Council

under

Department of the Navy  
Bureau of Ships Contract NObs-72046  
BuShips Index No. NS-731-036

Washington, D. C.  
National Academy of Sciences-National Research Council  
November 10, 1960

## ABSTRACT

Steel plates processed according to a conventional and controlled (low finishing temperature) rolling practice were studied to establish reasons for a superior notch toughness in the controlled-rolled product. The lower transition temperature (Charpy V-notch 15 ft-lb) in plates investigated is derived largely from a smaller ferrite grain size. Experimental evidence was also obtained to indicate that a part of the improvement results from a microfissuring in the plane of the plate at the notch root, with the effect that stress triaxiality is relieved and transition temperature depressed. The origin of the flaws responsible for the fissures was not determined with certainty, but there was good indication that they were simply inclusions in a fiber structure too fine in scale for observation with normal metallographic techniques. The criteria presented for microfissuring were: (1) a flaw structure dispersed on a scale no greater than the size of the plastic volume from which the brittle crack originated; (2) a ratio of the critical fracture stress in thickness (Z) to rolling (R) direction no greater than about  $1/2$ . The necessary fracturing anisotropy was favored by more intense fibering (lower  $\sigma_Z$ ) and finer grain size (higher  $\sigma_R$ ). The criteria were most nearly satisfied by controlled-rolled plate. Correlations between  $\sigma_Z$  and visible inclusion content showed the decrease in  $\sigma_Z$  to be paralleled by more elongated inclusions, as if visible changes are indicative of changes in the fine-scale fiber structure.

## CONTENTS

	<u>Page</u>
Introduction . . . . .	1
Materials . . . . .	3
Source . . . . .	3
Metallography . . . . .	3
Transition Temperatures . . . . .	4
Fracturing Anisotropy . . . . .	7
Nonmetallic Inclusions . . . . .	8
Low Temperature Tensile Deformation . . . . .	11
Procedures . . . . .	11
Fracture Observations . . . . .	15
Discussion . . . . .	18
Summary and Conclusions . . . . .	22
Acknowledgments . . . . .	23
References . . . . .	23
Appendix . . . . .	26

SR-147 PROJECT ADVISORY COMMITTEE  
"Mill Rolling Practice"  
for the  
COMMITTEE ON SHIP STEEL

Chairman:

T. S. Washburn  
Manager, Quality Control Department  
Inland Steel Company

Members:

J. L. Giove  
Chief Metallurgist  
U. S. Steel Corporation

J. R. LeCron  
Bethlehem Steel Company

T. T. Watson  
Manager, Metallurgical Division  
Lukens Steel Company

Cyril Welis  
Metals Research Laboratory  
Carnegie Institute of Technology

## INTRODUCTION

In general, processing materials by plastic deformation produces structural changes and, therefore, changes in mechanical properties. An example of interest is the hot rolling of steel at lower-than-normal temperatures, in the austenite and ferrite region. Such processing finds some use in the production of ship plate, and, as practiced with regulated temperature-reduction programs, has been termed controlled rolling. Improved notch toughness is attributed to controlled-rolled plate,<sup>1</sup> yet little in the way of a basic explanation for the improvement has been given in the literature.

Various structural differences could contribute to the superior properties. Finer grain size from lower finishing temperature would be expected to be one of the most important. Several investigations have been made of the dependence of transition temperature on ferrite grain size. Barring complication from subgrain or Widmanstätten structure,<sup>2-5</sup> the decrease is 8-15 C per ASTM grain-size number.<sup>4-7</sup>

A more strongly developed fibering or laminated condition is another difference that might contribute to improved notch toughness. Mechanical fibering commonly associated with ferrite banding and alignment in the direction of working of inclusions or other phases is the type to be considered. Crystallographic fibering or preferred orientation as found in hot-rolled plate should be much less significant. Because of this "lamination," properties relating to fracture are generally lower when measured across the fiber; as a common example, resistance to fracture over a surface in the plane of a rolled plate is practically always the least, with the greatest resistance being measured along the rolling direction and an intermediate level in the transverse direction. The more obvious fiber elements are reasonably expected to contribute to a fracturing anisotropy.<sup>8-12</sup> However, in work by Backofen et al,<sup>13, 14</sup> fracturing anisotropy was clearly demonstrated in a variety of relatively pure metals and single-phase alloys. It was concluded that wrought metals in general are characterized by a structure of highly aligned submicroscopic and crack-like flaws. The detailed nature of the structure has not

been established, but one reasonable view is that the flaws are simply very small inclusions which are not detected by usual metallographic examination.

The presence of a fiber structure might be expected to depress transition temperature only when fracture occurs in the presence of triaxial stress with cracking across the fiber. Then, as suggested by Soete<sup>15</sup> and Matton-Sjöberg,<sup>16</sup> tensile stress over the weakest plane may become sufficiently high to produce cracking or fissuring at right angles to the main crack path. The result would be some relief of the triaxiality, which acts to elevate transition temperature.

A number of experiments have been made in the past relating to this view. Matton-Sjöberg<sup>16</sup> compared two fine-grain steels and found a lower transition temperature consistent with narrower ferrite banding, although he pointed out at the same time the difficulty of separating such an effect from one caused by slag inclusions. Matton-Sjöberg and others<sup>17, 18</sup> as well have also established a dependence of transition temperature on the orientation of specimen and notch in a given plate. Different results were obtained, however, in a study by Owen, Cohen, and Averbach<sup>19</sup> with a coarse-grain steel showing broad ferrite banding. In that work, the Charpy-V 15 ft-lb transition temperature was insensitive to banding, and there was no evidence of anisotropy in this property. Inconclusive experiments by Mangio and Boulger<sup>20</sup> give another example of attention focused only on coarse-scale structure; these followed a suggestion from Orowan<sup>21</sup> that transition temperature might be lowered by artificially generating weak planes parallel to the rolled surface. Accordingly, plates were prepared by pack-rolling oxidized sheets and by intermittent casting to produce oxidized layers in the ingot.

A preoccupation with coarser details of structure has been common to all such work. As a result, the current experimental basis for appraising any effect of fissure formation on transition temperature still seems quite inadequate. For elements of fiber to be at all effective, they must be sufficiently small and finely distributed to compare in size with the small plastic volume beneath a notch or crack in which the brittle failure originates. The fine-scale flaw struc-



ture referenced previously, and generally characteristic of wrought material, would appear able to satisfy this requirement; the larger and more obvious inclusions and regions of banding would not. It was the principal aim of this research to separate, if possible, these effects of grain-size and fibering on ductile-to-brittle transition. In this way it was hoped that an explanation could be found for all of the improved notch toughness to be expected of "controlled-rolled" plate.

### MATERIALS

Source: Plates were produced by the Royal Netherlands Blast Furnace and Steel Works, Ltd. Two different analyses were included; these are given in Table I.

TABLE I. CHEMISTRY AND DESIGNATION OF TEST MATERIALS

<u>Designation</u>	<u>C</u>	<u>Mn</u>	<u>Si</u>	<u>P</u>	<u>S</u>
H, h	0.15	1.18	0.03	0.017	0.026
L, l	0.19	0.74	0.04	0.017	0.028

H and L were 1-1/2 in. thick; h and l were 3/4-in. thick. Taking adjacent ingots from the same charge, one was rolled in a conventional manner (designated S), while the other was controlled-rolled (designated C) with the last 30-35% of the reduction in the two-phase region and with a finishing temperature of 720 C. The detailed rolling schedule is shown in the Appendix. Most tests were carried out on HS- and HC- plates.

Metallography: Ferrite grain size was determined by linear analysis in both the rolling (R) and thickness (Z) directions. Since the grains were not equiaxed, the average grain diameter has been represented as  $\bar{d} = \sqrt{d_R d_Z}$ . The banding ratio was defined as the ratio of free ferrite path in the rolling direction to that in the thickness direction. Care was taken to compute the ratio only

after sufficient counting had taken place to insure that the percentage of ferrite (or pearlite) was the same (within 0.5%) in both directions. With this procedure, the ferrite and pearlite banding ratios are identical.

Results of the grain-size determinations are given in Table II.

TABLE II. FERRITE GRAIN SIZE FROM LINEAL ANALYSIS

	HC	HS	hC	hS	LC	LS	lC	lS
ASTM No.	8.5	7.5	9.5	8.6	8.2	6.7	9.2	7.8
$d_R/d_Z$	1.26	1.14	1.35	1.25	1.28	1.19	1.33	1.19

These measurements show that an important effect of controlled rolling in the plates under study was a reduction in ferrite grain size by about one ASTM Number for the high manganese (H, h) and 1.5 for the low (L, l). From Fig. 1, the banding ratio is seen to vary in an essentially inverse way with grain size, banding being more pronounced in the steel of finer grain size, irrespective of rolling process. Although the ratio is about 1.4 for the coarsest grain size, the structure would be rated non-banded from visual examination. Another trend in the structures is the nearly direct proportionality between ferrite grain size and ferrite patch size, shown plotted in Fig. 2. In the coarse-grain structures (LS and lS), however, patch size is smaller than predicted by the trend; this deviation is interpreted as marking the start of a change towards a structure of Widmanstätten type, even though there was no direct visual indication of such a change.

Transition Temperatures: A lower transition temperature in all C-plates is to be expected from Table II. If a factor in addition to grain size is contributing, however, a different grain-size dependence of transition temperature in C- and S-plates could be expected. Accordingly, the various heat treatments in Table III were carried out to alter ferrite grain size of HS and HC; all were terminated by furnace cooling. The resulting structures were banded with no indication of Widmanstätten structure. Charpy-V 15 ft-lb transition temperatures were determined by testing 25-30 specimens for each grain size with results as shown in Fig. 3\* For HS,

---

\*Specimens in rolling direction; notch in thickness direction.

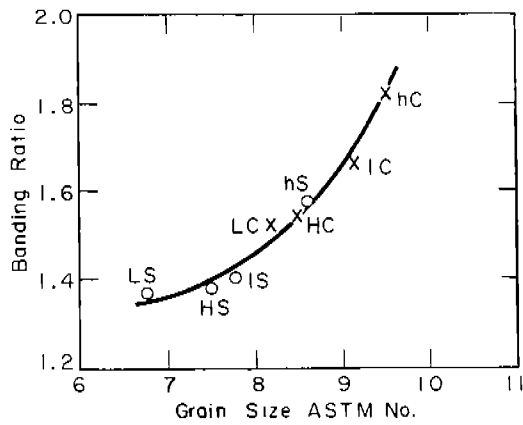


Fig. 1. Dependence of banding ratio on grain size. C: controlled, S: conventionally rolled. Trend not influenced by rolling practice.

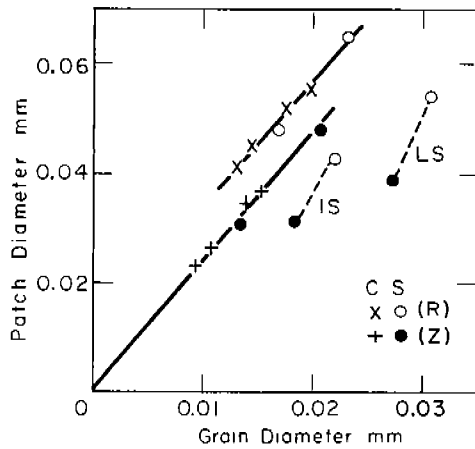


Fig. 2. Relationship between ferrite patch size and mean grain diameter from measurements in thickness (Z) and rolling (R) directions. Only coarse-grain IS and LS, low Mn and conventionally rolled, do not fit pattern.

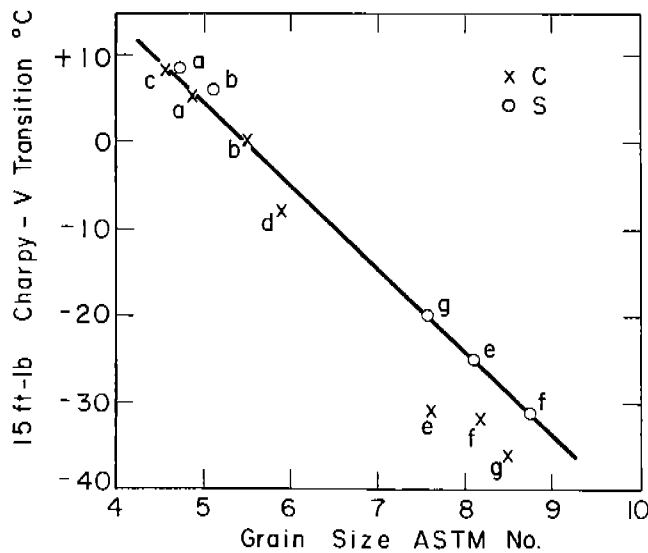


Fig. 3. Grain-size dependence of 15 ft-lb Charpy-V transition temperature determined after various heat treatments on plate HC and HS. Letters indicate treatments listed in Table III.

TABLE III. TREATMENTS OF HS AND HC FOR CHARPY TESTS

<u>Treatment</u>	<u>T (°C)</u>	<u>Time</u>	<u>Thickness</u>
a	1200	3 hr	full-plate
b	1100	3 hr	"
c	1050	24 hr	"
d	900	24 hr	"
e	900	1 hr	"
f	870	5 min	11 mm
g	----- as received-----		

the slope is 10 C/ASTM Nq; for HC, it is > 10 C/ASTM No. Two features are of special interest: With coarse grain size from prolonged high-temperature annealing, transition temperature is about the same; for finer grain size, however, which is more characteristic of the as-rolled product, HC has the lower temperature. A conclusion is that some amount (approximately 6 C) of the difference between as-rolled HC and HS is the result of an extra-grain-size effect.

These measurements on as-rolled HC and HS and other independent measurements are compared with good agreement in Table IV. Transition temperatures

TABLE IV. CHARPY V-15 TRANSITION TEMPERATURES OF HC AND HS

<u>Source</u>	<u>HC</u>	<u>HS</u>
This work	-36 C	-20 C
Producer	-35 C	-17 C
New York Naval Shipyard	-36 C	-20 C

of the other plates as determined by the producer are plotted against grain size in Fig. 4. Here it is seen that the value for LS does not compare well with that for LC. However, other tests at the New York Naval Shipyard give values of 1°C (LS)

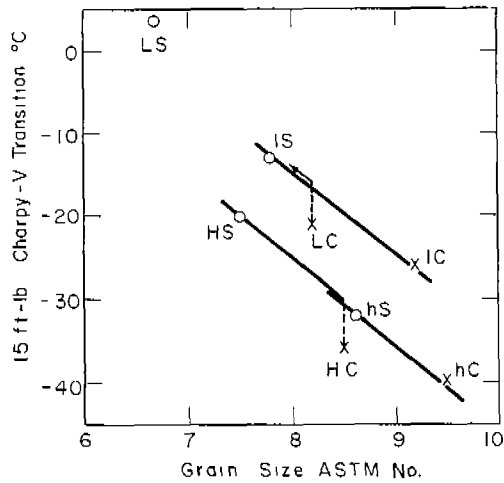


Fig. 4. Transition temperature versus grain size for all as-rolled material.

and -15 C (LC) for a difference of about 10 C/ASTM No. Similarly, for both sets of 3/4-in. thick plates, the differences in transition temperature correspond to 10 C/ASTM No. Such differences can be attributed entirely to grain size and are considered later in the discussion.

Fracturing Anisotropy: Information about fracturing anisotropy was obtained at room temperature with tension tests on specimens of 0.125-in. dia. gage section taken along rolling (R) and thickness (Z) directions in all plates. Samples of HC and HS were also heat treated to obtain differences in grain size and degrees of banding. A pronounced banding followed furnace cooling with virtually none after air cooling. Fracture stress in the Z-direction was determined only with some difficulty. The break was not abrupt as in the rolling direction. Rather, there was a gradual tearing with cracks in the rolling plane being formed soon after yielding. Initial strain hardening was essentially the same in both R- and Z-directions, however. Therefore, a Z-direction fracture stress,  $\sigma_Z$ , was computed by measuring fracture strain at the minimum section on a broken Z-specimen and taking the associated stress from the true stress-strain curve in the R-direction. Such a procedure was the least subjective and still gave values, although on the high side, that were reasonably close to a true fracture stress. All results are summarized in Fig. 5, where each point represents the average of 3 tests.

The slope of the  $\sigma_R$  vs  $d^{-1/2}$  line,  $8400 \text{ psi/mm}^{-1/2}$ , is in good agree-

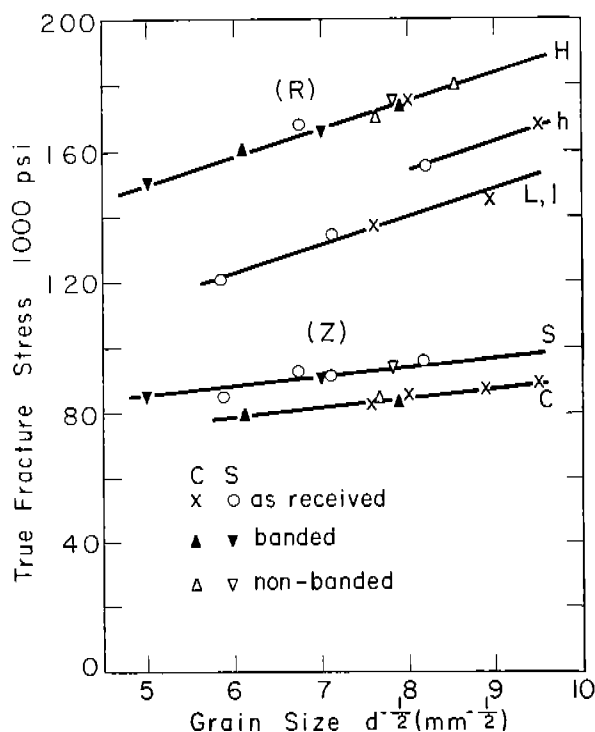


Fig. 5. True tensile fracture stress at 20 C in rolling (3 upper plots) and thickness direction (2 lower plots) as a function of ferrite grain size and with different degrees of banding.

ment with a value found by Heslop and Petch.<sup>7</sup> In the thickness direction, the slope is about  $2400 \text{ psi/mm}^{-1/2}$ , which is closer to the grain-size dependence of yield stress. At equal grain size,  $\sigma_Z$  is smaller for C-plates, but there is no systematic difference between banded and unbanded structures. Thus fracturing anisotropy is not influenced by the intensity of ferrite banding.

#### NONMETALLIC INCLUSIONS

Samples of all S-materials were analyzed at the Max-Planck-Institut für Eisenforschung.\* Two phases were found in each case, pure MnS and an oxide. Composition of the latter is given in Table V. The difference between HS and hS was unexpected, as both were obtained from the same charge although from different ingots. The oxide phase was the more ductile, being flatter and more elongated with sharper edges. When an inclusion contained both phases (duplex), the oxide appeared at the edges.

In investigating effects of rolling practice and heat treatment, an attempt was made to analyze length distributions. Inclusions were counted in an area of  $20\text{-}30 \text{ mm}^2$  on a surface defined by the rolling and thickness directions. Final polishing was done with a fine ( $< 1/4 \mu$ ) diamond paste. Four groups of different lengths were established: I: 0.01-0.02 mm; II: 0.02-0.04 mm; III: 0.04-0.08 mm; IV: 0.08-0.16 mm. Inclusions smaller than

\*Details of procedure are given in Ref. 22, 23, and 24.

TABLE V. INCLUSION ANALYSIS

Plate	Composition** (wt. %)				Total wt. % in. Sample
	SiO <sub>2</sub>	MnO	Al <sub>2</sub> O <sub>3</sub>	FeO	
HS	36	1	56	9	0.004
hS	75	-	18	7	0.009
LS	62	7	18	12	0.007
lS	67	4	18	11	0.012

\*\*Cr<sub>2</sub>O<sub>3</sub>, TiO<sub>2</sub>, MgO, CaO < 1% in all

TABLE VI. EFFECTS OF PROCESSING ON INCLUSIONS

Treatment	Ferrite Grain Size ASTM No.	Inclusion length ratio	
		Oxide	Duplex
HC as rec'd	8.5	1.00	1.00
HC 900 C - 24 hr - F. C.	6.3	0.85	0.85
HC 1050 C - 24 hr - F. C.	4.6	0.65	0.70
HC 1250 C - 24 hr - F. C.*	3.8+	0.35	0.55
HS as rec'd	7.5	0.85	0.95
HS 1250 C - 24 hr - F. C.	4.2+	0.30	0.55
hC as rec'd	9.5	1.25	0.85
hS as rec'd	8.6	0.95	0.85
LC as rec'd	8.2	1.10	0.80
LS as rec'd	6.7	0.80	0.80
lC as rec'd	9.2	1.40	0.80
lS as rec'd	7.8	1.15	0.75

\*Furnace-cooled with retarded cooling rate: 900 C to 700 C in 12 hr  
 +Widmanstätten structure

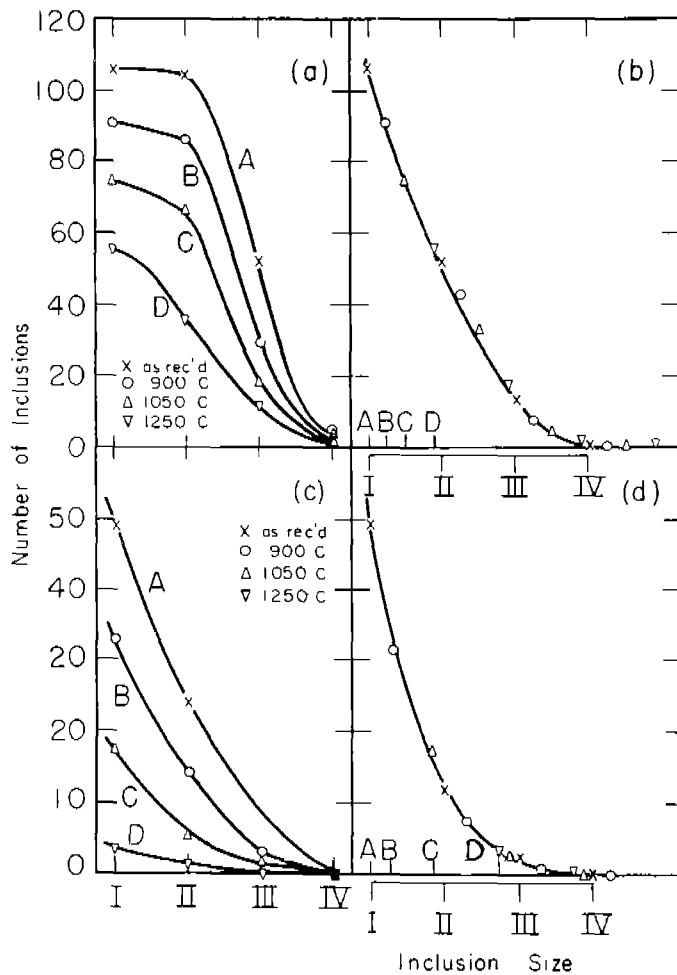


Fig. 6. Distribution of duplex (a, b) and oxide (c, d) inclusions in HC plate after various heat treatments (Table VI). Size groups: I: 0.01--0.02 mm; II: 0.02--0.04 mm; III: 0.04--0.08 mm; IV: 0.08--0.16 mm. Area represented is 10 mm<sup>2</sup> defined by rolling direction and thickness direction. Measurements on the plane surface are shown in (a) and (c); adjustments for volume distribution (see text) are made in (b) and (d).

those of Group I could not be recounted for verification within reasonable limits, probably because of difficulty in retaining them through polishing. Sizes greater than Group IV were also neglected, being too infrequent to be reproduced well. The counting was carried out for all plates in the as-received condition and also for HS and HC after several annealing treatments (see Table VI). An example based on as-received and annealed HC is given in Figs. 6a and 6c, where the distribution is seen to shift towards the left with annealing. Inclusions clearly become spheroidized, the oxides at a somewhat greater rate.

The number counted on a plane section does not represent distribution in volume without some correction for the fact that the probability of cutting an inclusion will diminish with its width. Assuming width and length to be proportional, volume distribution was estimated by multiplying each size group in a



10 mm<sup>2</sup> area by the factor: 1/1 for Group I, 1/2 for Group II, 1/4 for Group III, and 1/8 for Group IV. Counting data for all materials were adjusted accordingly.

Further comparisons were then made assuming a constant number of inclusions and a similar distribution pattern; the only difference considered was that inclusions in one sample may be longer by a certain factor. This length factor could be obtained from the horizontal separation between plots of number vs logarithm of length, which corresponds to the logarithm of the length ratio. Measurements plotted in Figs. 6a and 6c are treated this way in Figs. 6b and 6d where all curves superimpose quite well; length ratios are obtained from the different locations on the abscissa to which the curves have been displaced. Complications are, of course, introduced by differences in chemical analysis; specifically, larger oxide content resulting in a larger number of inclusions would be interpreted as longer inclusions. However, it should be possible to evaluate, at least approximately, effects of annealing and rolling practice if comparisons are made only between the C- and S-plates of any particular pair and if it is assumed that there are no major differences between analyses of controlled and conventionally rolled plate.

Inclusion length ratios, taking as-received HC as 1.00, are listed in Table VI. Conclusions to be drawn are:

- (a) Comparing C- and S-plates, oxides were about 30% longer in C. Difference between HC and HS was only 15%, possibly owing to the higher alumina content.
- (b) Differences between duplex inclusions in as-rolled plates were negligible. The deformation of sulfides was apparently not affected by rolling practice.

#### LOW TEMPERATURE TENSILE DEFORMATION

Procedures: Tensile tests were made at temperatures as low as 58 K (-215 C) to investigate fracturing anisotropy as the ductile-brittle transition is approached. Materials were the differently treated HC and HS listed in Table VI. Testing was carried out in an apparatus consisting essentially of a long rod sliding within a tube and positioned vertically in the neck of a liquid nitro-

gen or helium storage vessel. The specimen was gripped between the bottom of the tube and the lower end of the rod while the apparatus was mounted in a hydraulic testing machine. The upper end of the rod was attached through a spherical seat to one crosshead and the upper end of the tube fastened to the other. A round, horizontal cross-bar projected through a universal-type joint in the lower grip for locking the specimen to the tube; the assembly of rod, grips, and specimen was passed down through a slotted plate closing the tube so that by turning 90° and retracting, the bar made contact with the under side of the plate. A linkage between the grips kept a broken specimen from dropping into the vessel. There was no need to move the tube during a series of tests as specimens could be changed by turning the central rod to free the cross-bar and then withdrawing the rod from the neck. The tests were made at a crosshead rate of 0.05 in./min.

Specimens from both thickness and rolling direction were 1-1/2 in. long, with a gage length of 7/8 in. and a diameter of 0.250 in. True fracture stress was calculated from the diameter at fracture as measured with an optical comparator and the load reading at which an audible click indicated fracture. Unlike specimens of 0.125 in. diam., fracture occurred at a fairly well-defined stress even in the thickness direction, indicating that the gradual tearing-apart process is important only with small diameter.

A flow of gas up through the neck for cooling the specimen was obtained by blowing tank gas ( $N_2$  or He) into the liquid. A copper-constantan thermocouple was attached to each specimen near the center of the gage length and, with some experience, temperature could be controlled to  $\pm 1^\circ C$  by manually adjusting the flow rate. The lowest temperature conveniently obtained with nitrogen was  $-182^\circ C$ ; below this, helium was used. Between  $-182^\circ C$  and about  $-205^\circ C$ , normal evaporation of the helium cooled the specimen to such an extent that the room-temperature gas had to be blown in above the liquid level. Constant temperature was maintained in all cases for 5-15 min before starting a test. The total time required for one test was 40-60 min.

Figures 7-12 represent the temperature dependence of: true tensile fracture stress in both rolling,  $\sigma_R$ , and thickness,  $\sigma_Z$ , directions; lower yield stress,

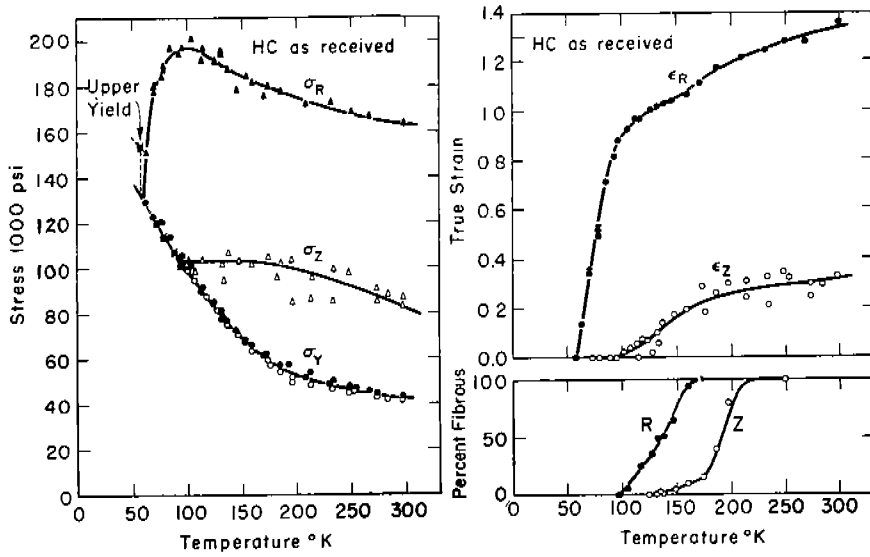


Fig. 7

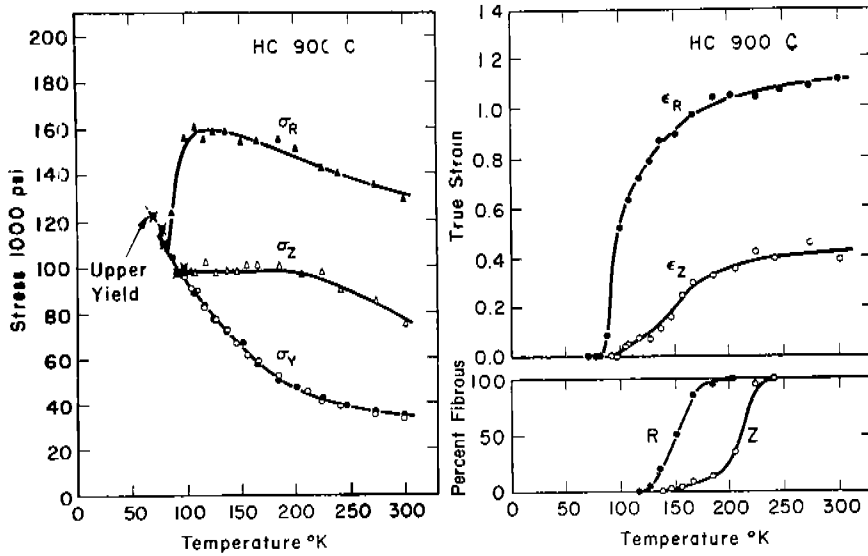


Fig. 8

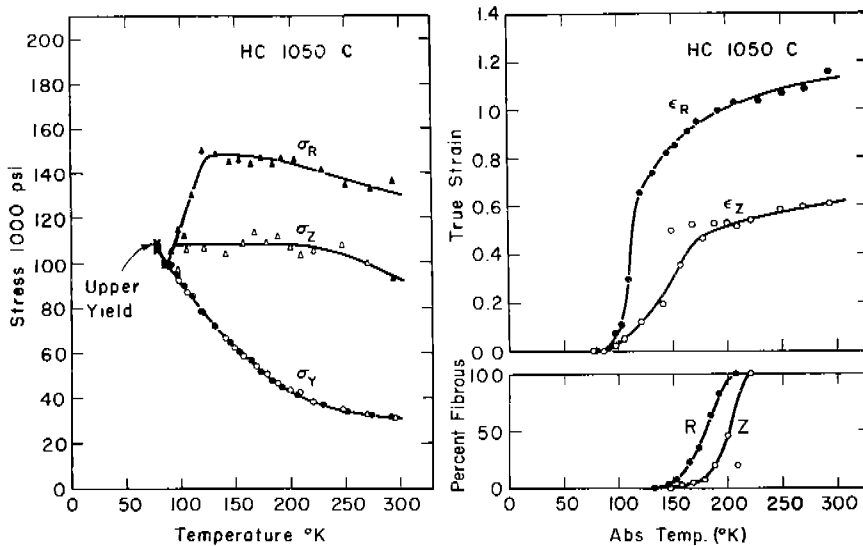


Fig. 9

Temperature dependence of true tensile fracture stress ( $\sigma_R, \sigma_Z$ ), yield stress ( $\sigma_Y$ ), fracture strain ( $\epsilon_R, \epsilon_Z$ ), and extent of fibrous area on samples from rolling (R) and thickness (Z) directions.

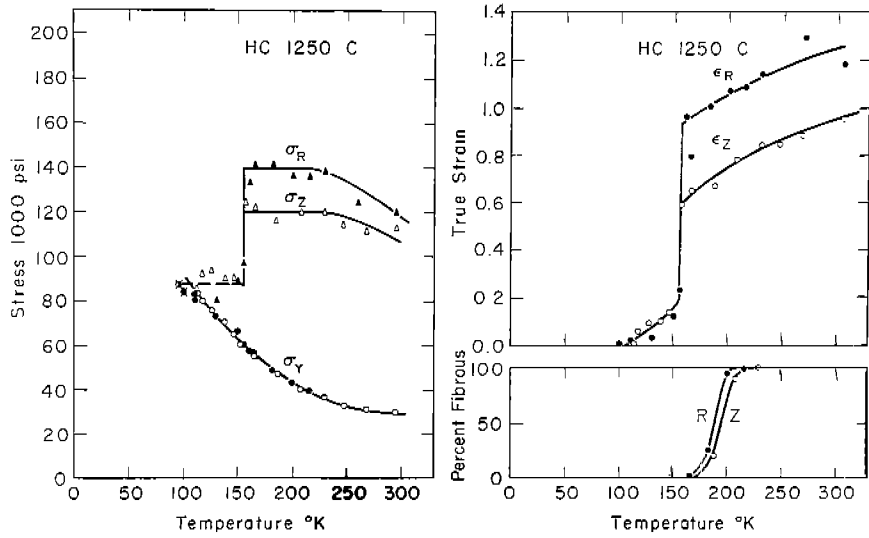


Fig. 10

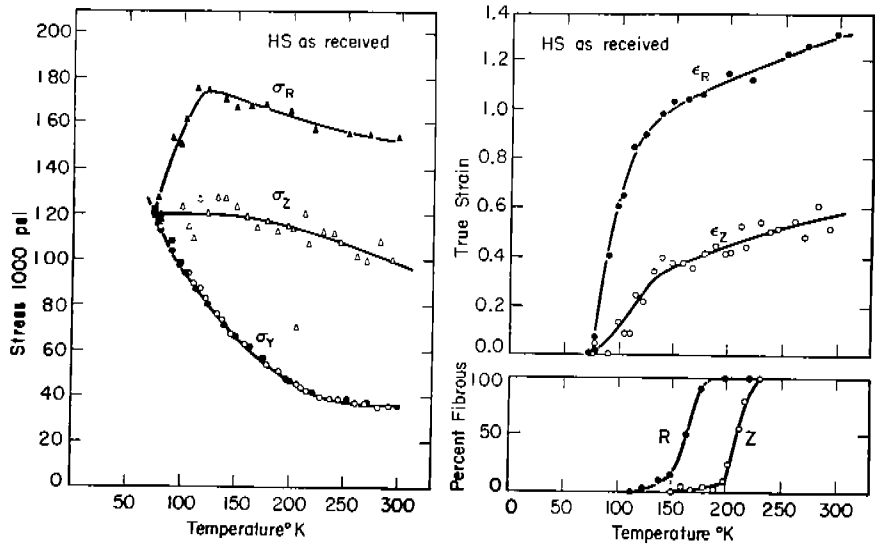


Fig. 11

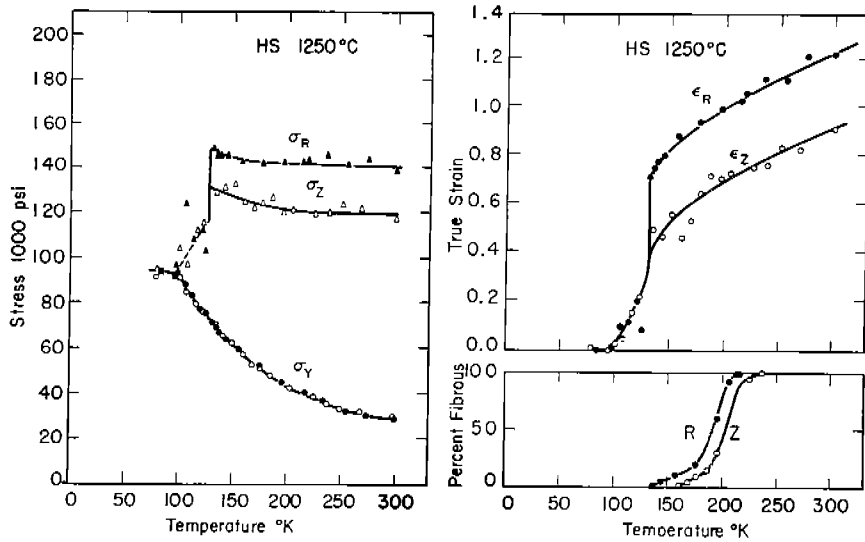


Fig. 12

Temperature dependence of true tensile fracture stress ( $\sigma_R$ ,  $\sigma_Z$ ), yield stress ( $\sigma_Y$ ), fracture strain ( $\epsilon_R$ ,  $\epsilon_Z$ ), and extent of fibrous area on samples from rolling (R) and thickness (Z) directions.



Fig. 13. Cracking around visible inclusions after yielding in a specimen (HS) from the thickness direction (500 X).

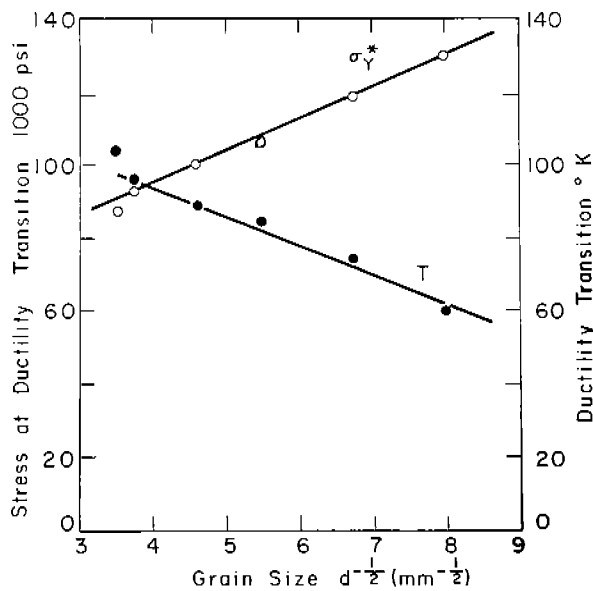


Fig. 14. Ductility transition temperature (intersection of  $\sigma_R$  and  $\sigma_Y$  curves in Figs. 7--12) and corresponding stress  $\sigma_Y^*$  as a function of grain size. Trend is insensitive to rolling practice.

$\sigma_Y$ ; and true tensile fracture strain,  $\epsilon_R$  and  $\epsilon_Z$ . These figures also indicate the extent of fibrous area on fracture surfaces of R- and Z- specimens, visually estimated.

Fracture Observations: At low temperatures, as at room temperature, freely visible surface cracks normal to the stress axis in Z- specimens appeared after yielding. Cracks were not found when fracture occurred at the upper yield point; therefore such cracking must be associated with plastic deformation. Microscopic examination showed that the cracks originated at inclusions,

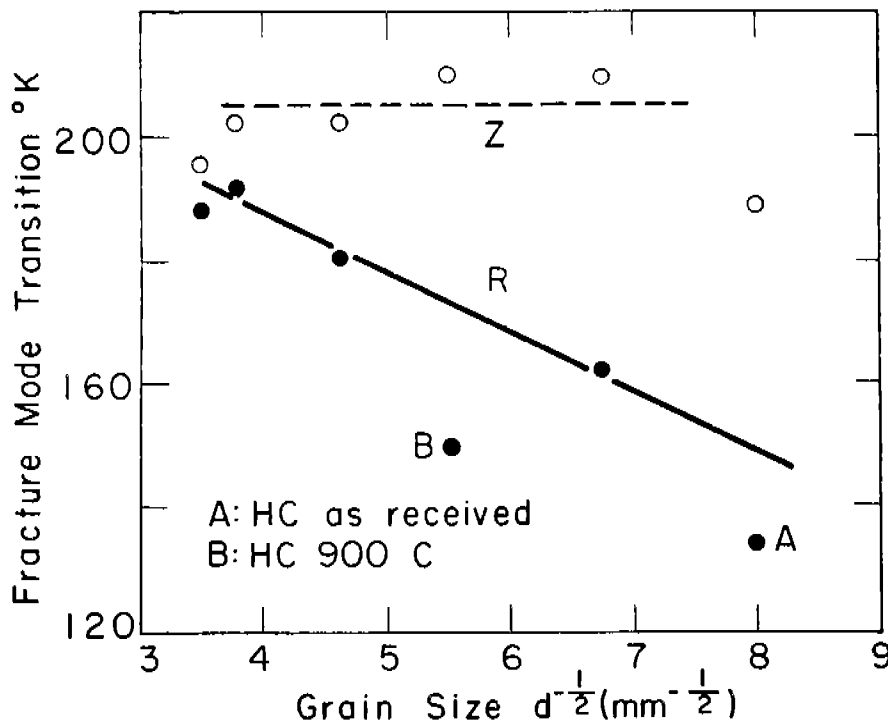


Fig. 15. Grain-size dependence of temperature for 50% fibrous fracture from Figs. 7--12. Differences indicated are consistent with Fig. 3.

as in Fig. 13. Apparently the path of ductile fracture follows along many of these damaged areas, for numerous inclusions may be seen in the fracture surfaces of Z-specimens.

Variation with grain size of the ductility transition temperature, defined as the intersection of  $\sigma_R$  and  $\sigma_Y$  curves, and the corresponding  $\sigma_Y^*$  are plotted in Fig. 14. There is no difference between conventional and controlled-rolled specimens in this regard. A fracture-appearance transition temperature was also defined by 50% fibrous fracture area. Its dependence on grain size is shown in Fig. 15, in which the line is drawn with the same slope as in Fig. 14. Here the lower levels of HC-plate as-received and annealed at 900 C suggest a depression in transition temperature for some extra-grain-size reason even more distinctly than in the 15 ft-lb Charpy transition (Fig. 3).

The spread in  $\sigma_Z$  measurements on as-received specimens seems to represent not experimental error but rather a material characteristic, for it is reduced by annealing. A few as-received specimens, especially of HS, broke at abnormally low stresses, even below the yield point. When this happened, an unusually large inclusion could always be found in the fracture. Thus the

very large, sharp-edged (as-rolled) inclusions do occasionally initiate fracture, but there is no indication that they are generally important in this respect. Over a range of low temperatures,  $\sigma_Z$  is essentially constant (Figs. 7-12), even as the fracture mode changes from largely ductile to brittle and the fracture path no longer follows inclusions. This suggests a critical stress criterion for these conditions, with both ductile and brittle modes sharing a common initiation process which determines the level of  $\sigma_Z$ .

As the ductility transition temperature is approached, both  $\sigma_R$  and  $\epsilon_R$  drop rapidly, but they do so for most specimens without indication of the discontinuous or bimodal fracturing suggested in results obtained by Wessel<sup>25</sup> and Hahn et al.<sup>26</sup> The clearest example is given by HC as-received for which the ductility drop occurred at liquid nitrogen temperature. A large spread in  $\epsilon_R$  would be expected for a discontinuous change. Yet at liquid nitrogen, three tests giving an intermediate ductility level were closely reproduced (Fig. 7). Only for HS and HC annealed at 1250 C was the change so sharp that fracturing could, with some confidence, be interpreted as bimodal. The temperature difference between the abrupt drop in ductility and the ductility transition was larger for HC, which was cooled from the annealing temperature at a slower rate and had a larger grain size.

Large differences in fracturing anisotropy, defined as  $\sigma_{Z(\max)}/\sigma_{R(\max)}$  from Figs. 7-12, are listed in Table VII. These derive from at least two sources:

TABLE VII. EFFECT OF PROCESSING ON FRACTURING ANISOTROPY

Plate	Treatment	$\frac{\sigma_Z (\max)}{\sigma_R (\max)}$
HS	1250 C - 24 hr - F.C.	0.88
HC	1250 C - 24 hr - F.C.	0.87
HC	1050 C - 24 hr - F.C.	0.72
HS	as rec'd	0.69
HC	900 C - 24 hr - F.C.	0.61
HC	as rec'd	0.52

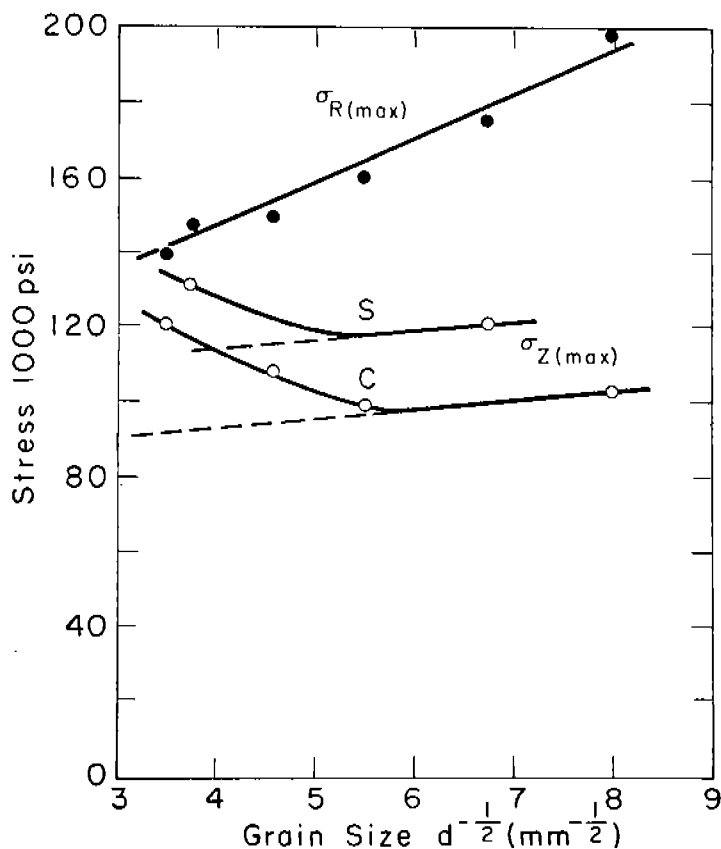


Fig. 16. Dependence on grain size of maximum fracture stresses from Figs. 7--12. Two reasons for reduced fracturing anisotropy are demonstrated: lower  $\sigma_{R(max)}$  with increasing grain size and increased  $\sigma_{Z(max)}$  from high temperature annealing.

differences in inclusion distribution and in grain size. The grain-size effect is illustrated by room-temperature measurements (Fig. 5) showing  $\sigma_Z/\sigma_R$  to decrease with reduction in grain size because of  $\sigma_R$  increasing more rapidly than  $\sigma_Z$ . Effects of the annealing treatments on both inclusions and grain size are reflected in Fig. 16. A Widmanstätten structure in the HC- and HS-specimens annealed at 1250 C results in a grain-size uncertainty. However, it is still clear that a consequence of prolonged annealing is an increase in  $\sigma_Z$  superimposed on the room-temperature trend (Fig. 5, slope = 2400 psi/mm $^{-1/2}$ ) for as-rolled and normalized specimens. This increase follows closely the spheroidizing of inclusions described

in Fig. 6 and Table VI. Unfortunately, detailed comparisons between HC and HS are difficult because it is uncertain that they have the same inclusion analysis. Nevertheless, lower  $\sigma_{Z(max)}$  for HC does correlate with more elongated inclusions in the controlled-rolled plate, which should contribute to lower fracture stress in the Z-direction. Perhaps the reasonable view is that changes in the more obvious inclusions serve only as qualitative indicators of changes in the fine-scale flaw structure so important to fracturing anisotropy.

#### DISCUSSION

The experiments reported here have demonstrated an effect of rolling



practice on fracturing characteristics. They have also shown that fracturing anisotropy does not result from ferrite banding, but rather, there is evidence that a structure of elongated flaws is the primary cause. The further indication is that such a condition may contribute, along with reduced grain size, to a lowering of transition temperature by controlled rolling. The argument is that outlined earlier.

With a standard Charpy bar as the example, deformation beneath the notch produces a tension stress  $\sigma_3$  across the weak plane parallel to the plate surface;  $\sigma_3$  is only a fraction  $q$  of the axial stress  $\sigma_1$ , or  $\sigma_3 = q\sigma_1$ . A separation or fissuring occurs in this plane before a brittle crack forms if  $\sigma_3$  reaches the level of Z-direction fracture stress  $\sigma_3^*$  before  $\sigma_1 = \sigma_1^*$ , the fracture stress in the R-direction. Therefore, the requirement for fissuring is that  $\sigma_3^*/\sigma_1^* < q$ . The fissure must lower both hydrostatic and axial stress and thus reduce the tendency for brittle fracture. Recent work by Hendrickson, Wood, and Clark<sup>27, 28</sup> can also be interpreted in support of the argument and used in a more specific statement.

It was shown that brittle fracture in both notched tension specimens and Izod bars occurred as  $\sigma_1$  reached a critical level  $\sigma_1^*$  at the elastic-plastic boundary of a small plastic zone beneath the notch. In general,  $\sigma_1 = K\sigma_y$ ;  $K$  depends upon notch geometry, increasing with distance beneath the surface to a maximum at the boundary, and  $\sigma_y$  is fixed by prevailing conditions of structure, temperature, and stress rate. At the transition temperature, the plastic zone is on the verge of propagating across the section, and  $\sigma_1^* = K_m \sigma_y^*$ , with  $K_m$  having the largest possible value for given geometry and method of loading. A corollary is that under fixed conditions the ductile-brittle transition may be characterized by a critical value of yield stress,  $\sigma_y^*$ . In the notched Izod and Charpy specimen,  $K_m = 2.4$ . For plane-strain deformation,  $\sigma_3 = \frac{\nu(2K-1)}{K} \sigma_1$ , where  $\nu$  is Poisson's ratio. Therefore, at the transition temperature,  $\sigma_3 \simeq 0.5\sigma_1^*$ , and here  $q$  is a maximum at  $q_m = 0.5$ . Below the transition temperature,  $\sigma_1^*$  is still reached at the elastic-plastic boundary. Now, however,  $\sigma_1^* = K'\sigma_y'$ , where  $\sigma_y' > \sigma_y^*$ , so that  $K' < K_m$ , with the two results that the boundary lies nearer to

the notch root and  $q' < q_m$ . Accordingly, the fissuring criterion,  $\sigma_3^*/\sigma_1^* < q$ , is most likely to be satisfied around the transition temperature since here  $q$  is maximum. Fissuring could also be expected at lower temperatures, although  $q$  becomes less, so that eventually  $\sigma_3$  may not reach  $\sigma_3^*$  before  $\sigma_1 = \sigma_1^*$ . In these terms, the effect of fissuring is to lower the constraint, expressed by  $K$ , in a small volume around the plastic-elastic boundary. The result with the given testing method is that lower temperature is necessary to obtain higher  $\sigma_y$ , thus compensating for reduced  $K$  in reaching  $\sigma_1^*$ .

The  $\sigma_z/\sigma_R$  values in Table VII indicate that fissuring at and near the transition temperature might be expected for some treatments. Values of  $\sigma_1^*$  for these steels are unknown and apparently cannot be measured under pure tensile loading. In any event, the experimental  $\sigma_{R(max)}$  is perhaps not far below  $\sigma_1^*$ . The existence of  $\sigma_3^*$  must be postulated, although the idea seems a reasonable one;  $\sigma_z$  is relatively insensitive to temperature over the lower end of the range, and the level on approaching intersection with the  $\sigma_y$  curve ( $\sigma_{z(max)}$ ) may then be viewed as an approximation to  $\sigma_3^*$ . Therefore, the measurements of  $\sigma_{z(max)}/\sigma_{R(max)}$  would seem reasonable (high) approximations to  $\sigma_3^*/\sigma_1^*$ . On this basis, treatments giving the smallest values of  $\sigma_z/\sigma_R$  have the highest probability of fissuring. Accordingly, the materials in order of decreasing tendency to develop fissures may be read from Table VII starting with the most likely, controlled-rolled HC as received ( $\sigma_{z(max)}/\sigma_{R(max)} = 0.52$ ), and going to the least, HS annealed at 1250 C ( $\sigma_{z(max)}/\sigma_{R(max)} = 0.88$ ). Of these, the two materials with lowest ratios also have the lowest transition temperatures if comparisons are made after adjustment for differences in grain size (Fig. 3).

The basic requirement in this argument, a finely dispersed flaw structure, has been stressed. Evidence for such a structure exists, and supporting observations were made in the present work. Figure 17 represents the fracture surface directly beneath the notch in a Charpy specimen breaking with energy absorption of 6 ft-lb. Normally this fracture would be classed as 100% brittle, yet a microfissuring in the rolling plane is clear over a region of a size (2-5  $\mu$ )



Fig. 17. An observation of the fracture surface of microfissuring beneath the notch in a brittle Charpy specimen (HC) (2000 X).

consistent with the plastic volume that develops before the brittle crack. Microfissures at the notch root could also be observed in somewhat more ductile specimens, but these were rapidly obscured with increasing deformation.

The specimen in Fig. 17 happens to be HC as rolled; similar observations can be expected in other materials with properties favorable for fissure formation. Findings to date show only that microfissuring occurs; further study is necessary before variations in degree can be established and the origin of the fissures made clear. It seems a reasonable possibility that they result from very small inclusions. Although an intense fibering is important, it may not be a sufficient condition for microfissuring. It is clear from Figs. 5 and 16 that fine grain size also contributes to reduced  $\sigma_Z/\sigma_R$  through an increase in  $\sigma_R$ . In H-steels the probability of fissuring proved greatest, since higher  $\sigma_R$  was realized even for constant grain size. This would seem to be a reason for finding the microfissuring effect only in this material (Fig. 4).

In the heavily deformed regions, beneath surfaces of ductile fracture, cracks were clearly evident around practically every visible inclusion. These areas were sometimes connected to form a large crack lying in the rolling plane which might best be termed a macrofissure. Such fissures are relatively common in the ductile range where they do influence notched-bar energy absorption.

However, their spacing is too great compared with the size of the plastic volume at the notch root to act as efficient stress-relievers in the low energy-absorption range.

As a final observation, there is reasonable experimental support for the view that microfissuring can be involved in determining the level of notched-bar transition temperature. Grain size as well as the fibering necessary for microfissuring are both influenced by processing history. Therefore, critical evaluation of the effect of processing on notch toughness should consider both structural details; advantage may even derive from processing designed for control over both.

### SUMMARY AND CONCLUSIONS

1. The lower Charpy-V 15 ft-lb transition temperatures of controlled-rolled plates studied in this program result largely from smaller ferrite grain size. There is experimental evidence, however, that a part of the improvement may result from a microfissuring in the plane of the plate at the notch root; the effect is to relieve stress triaxiality and so depress transition temperature.

2. Microfissuring is not unique to controlled-rolled plate. Two requirements must be satisfied for its occurrence, regardless of processing history: (1) a flaw structure dispersed on a scale no greater than the size of the plastic volume from which the brittle crack originates; and (2) a ratio of the critical fracture stress in thickness (Z) to rolling (R) direction no greater than about 1/2.

3. Microfissuring may be seen beneath the notch root in Charpy specimens broken with little plastic deformation. The origin of flaws responsible for the fissures is not clear but may simply be inclusions too small for observation with normal metallographic techniques. Neither the visible inclusions, responsible for a macroscopic ductile fissuring, nor ferrite banding have an effect on transition temperature.

4. The ratio  $\sigma_Z/\sigma_R$  in tension over a range of temperatures extending down to the ductility transition is lowest for controlled-rolled plate in the as-rolled condition because of the low values of both  $\sigma_Z$  and grain size (giving high  $\sigma_R$ ).

5. Correlations between  $\sigma_Z$  and inclusion content show a decrease in  $\sigma_Z$  to be paralleled by more elongated inclusions, as if the visible changes are indicative

of changes in the fine-scale fiber structure. Annealing above 900 C gradually spheroidizes inclusions and is accompanied by marked increase in  $\sigma_z$ .

#### ACKNOWLEDGMENTS

This work has been done in a program sponsored by the Ship Structure Committee and under the guidance of a project advisory committee of the Committee on Ship Steel of the National Academy of Sciences-National Research Council. The authors are indebted to the Max-Planck-Institut für Eisenforschung for carrying out the inclusions extraction-analyses. They are also grateful to Behram Kapadia for experimental assistance throughout the work.

#### REFERENCES

1. Lightner, M. W., and Vanderbeck, R. W., "Factors Involved in Brittle Fracture," AISI Regional Meeting, Pittsburgh, November 28, 1956.
2. Josefsson, Åke, "Impact Transition Temperatures of Some Pearlite-Free Mild Steels as Affected by Heat Treatments in the Alpha Range," Transactions, AIME, vol. 200, pp. 652-659 (1954).
3. Danko, J. C. and Stout, R. D., "The Effect of Subboundaries and Carbide Distribution on the Notch Toughness of an Ingot Iron," Transactions, ASM, vol. 49, pp. 189-203 (1957).
4. Frazier, R. H., Boulger, F. W., and Lorig, C. H., "Influence of Heat Treatment on the Ductile-Brittle Transition Temperature of Semikilled Steel," Transactions, AIME, vol. 203, pp. 652-659 (1954).
5. Owen, W. S., Whitmore, D. H., Cohen, M., and Averbach, B. L., "Relation of Charpy Impact Properties to Microstructure of Three Ship Steels," The Welding Journal, vol. 22, pp. 503s-511s (1957).
6. Hodge, J. M., Manning, R. D., and Reichhold, H. M., "The Effect of Ferrite Grain Size on Notch Toughness," Journal of Metals, vol. 1, pp. 233-240 (1949).

7. Heslop, J., and Petch, N. J., "Dislocation Locking and Fracture in  $\alpha$ -Iron," Phil. Mag., vol. 2, pp. 649-658 (1957).
8. Kinzel, A. B., and Crafts, W., "Inclusions and Their Effect on Impact Strength of Steel," Transactions, AIME, vol. 95, pp. 143-173, 181-188 (1931).
9. Wells, C. and Mehl, R. F., "Transverse Mechanical Properties in Heat Treated Wrought Steel Products," Transactions, ASM, vol. 41, pp. 715-818 (1949).
10. Loria, E. A., "Transverse Ductility Variations in Large Steel Forgings," Transactions, ASM, vol. 42, pp. 486-498 (1950).
11. Welchner, J., and Hildorf, W. G., "Relationship of Inclusion Content and Transverse Ductility of Chromium-Nickel-Molybdenum Gun Steel," Transactions, ASM, vol. 42, pp. 455-473 (1950).
12. Watanabe, M., and Ideguchi, Y., "Anisotropic Properties of Rolled Steel and Experimental Analysis of Their Causes," Tech. Rep. Osaka Univ. Faculty of Engr., vol. 6, pp. 345-358 (1956).
13. Backofen, W. A., and Hundy, B. B., "Mechanical Anisotropy in Some Ductile Metals," Journal of Institute of Metals, vol. 81, pp. 433-438 (1952-53).
14. Backofen, W. A., "Mechanical Anisotropy in Copper," Transactions, ASM, vol. 46, pp. 655-674 (1954).
15. Soete, W., "Transverse Strength and Brittle Fracture," Journal of West of Scotland Iron and Steel Institute, vol. 60, pp. 276-293 (1952-53).
16. Matton-Sjöberg, P., "The Mechanism of Fracture in Impact Tests," Journal of West of Scotland Iron and Steel Institute, vol. 60, pp. 180-223 (1952-53).
17. Bagsar, A. B., "Notch Sensitivity of Mild Steel Plates," The Welding Journal, vol. 28, pp. 484s-506s (1949).
18. Puzak, P. P., Eschbacher, E. W., and Pellini, W. S., "Initiation and Propagation of Brittle Fracture in Structural Steels," The Welding Journal, vol. 31, pp. 561s-581s (1952).
19. Owen, W. S., Cohen, M., and Averbach, B. L., "The Influence of Ferrite Banding on the Impact Properties of Mild Steel," The Welding Journal, vol. 23, pp. 368s-377s (1958).

20. Mangio, C. A., and Boulger, F. W., "The Effect of Variations in Texture on Energy Absorption and Transition Temperature," Appendix A, An Appraisal of the Properties and Methods of Production of Laminated or Composite Ship Steel Plate (Ship Structure Committee Report Serial No. SSC-84), Washington: National Academy of Sciences-National Research Council, January 12, 1956.
21. Orowan, E., "Discussion," Appendix D, Ibid.
22. Klinger, P. and Koch, W., "Beiträge zur Metallkundlichen Analyse," Stahl u Eisen Verlag, 1949.
23. Koch, W., and Sundermann, H., "Elektrochemische Grundlagen der Isolierung von Gefügeb Bestandteilen in Stählen," Arch. Eisenhüttenwesen, vol. 28, pp. 557-566 (1957).
24. Koch, W., and Sundermann, H., "Magnetische Trennung Elektrolytisch Isolierter Gefügeb Bestandteile aus Metallischen Werkstoffen," Arch. Eisenhüttenwesen, vol. 29, pp. 219-224 (1958).
25. Wessel, E. T., "A Tensile Study of the Brittle Behavior of a Rimmed Structural Steel," Proceedings, ASTM, vol. 56, pp. 540-554 (1956).
26. Hahn, G. T., Averbach, B. L., Owen, W. S., and Cohen, M., "Micro-mechanism of Brittle Fracture in Low-Carbon Steel," The Welding Journal, vol. 38, Research Supplement, pp. 367s-376s (September 1959).
27. Hendrickson, J. A., Wood, D. S., and Clark, D. S., "The Initiation of Brittle Fracture in Mild Steel," Transactions, ASM, vol. 50, pp. 656-681 (1958).
28. Hendrickson, J. A., Wood, D. S., and Clark, D. S., "Prediction of Transition Temperature in a Notched Bar Impact Test," Transactions, ASM, Preprint No. 96, 1958.

APPENDIX

Rolling Schedule: Ingots were 80-3/4 in. in height, measuring 31-1/4 x 60-1/4 in. at the bottom and 29-1/2 x 59 in. at the top. Reduction consisted of rolling first to slabs: 98 x 55 x 9 in. for L and H plate, and 61 x 55 x 9 in. for l and h plate. With further rolling in a two-high mill, L- and H-slabs were reduced to 3-1/2 in. and 4-1/4 in., respectively, and l and h were reduced to 3 in. and 2-3/4 in., respectively. The S-plates were finished in a four-high mill according to more conventional practice, the temperature of the finishing pass being between 930 C and 970 C. The controlled-rolled C-plates were finished with the following schedule:

Pass No.	1	2	3	4	5	6	7	8	
Pass Temp.	>910°	890°	860°	830°	800°	770°	740°	720°	After finishing pass, cooling rate to 200 C
Plate	Thickness (in.)								
HC 1-1/2 in.	>2.25	2.08	1.93	1.80	1.67	1.56	1.46	1.46	16 C/min
LC 1-1/2 in.	>2.25	2.13	1.97	1.81	1.69	1.56	1.47	1.47	14 C/min
hC 3/4 in.	>1.20	1.10	1.02	0.93	0.85	0.77	0.72	0.72	16 C/min
lC 3/4 in.	>1.18	1.08	0.99	0.90	0.83	0.75	0.70	0.70	18 C/min



COMMITTEE ON SHIP STEEL

Chairman:

Professor John Chipman  
Head, Department of Metallurgy  
Massachusetts Institute of Technology

Vice Chairman:

Mr. M. W. Lightner  
Vice President, Research and Technology Division  
United States Steel Corporation

Members:

Professor C. S. Barrett  
Institute for the Study of Metals  
University of Chicago..

Mr. Paul Ffield  
Assistant Manager of Research  
Bethlehem Steel Company

Professor Maxwell Gensamer  
Professor of Metallurgy  
School of Mines  
Columbia University

Dr. J. R. Low, Jr.  
Metallurgy Research Unit  
Research Laboratory, General Electric Co.

Mr. T. S. Washburn  
Manager, Quality Control Department  
Inland Steel Company

Mr. T. T. Watson  
Director of Research  
Lukens Steel Company